

## The Coupled Logistic Map: A Simple Model for the Effects of Spatial Heterogeneity on Population Dynamics

ALUN L. LLOYD

Department of Zoology, University of Oxford, South Parks Road, Oxford OX1 3PS, U.K.

(Received on 3 August 1993, Accepted in revised form on 19 October 1994)

A simple model consisting of two diffusively coupled logistic maps is used to examine the effects of spatial heterogeneity on population dynamics. Examining the dynamic behaviour of the model using numerical methods, a wide range of behaviours are observed. It is shown that the coupling can stabilize individually chaotic populations, and that under different circumstances the coupling can cause individually stable periodic populations to undergo more complex behaviour. The system exhibits multiple attractors when the qualitative dynamics of the system depend on the initial conditions. Sudden changes in the structure of the attractors are seen for small changes in the parameters; these changes are known as crises. Transient and intermittent behaviours are observed. The implications of all these behaviours for populations are discussed. A linear coupling of the two maps is also considered which leads to counterintuitive behaviour, with chaotic dynamics being obtained by coupling two stable maps. This behaviour occurs because the coupling involves mixing of generations, and is therefore biologically unrealistic.

### 1. Introduction

Much attention has recently been focused on the effects of spatial heterogeneity on population dynamics (Kot, 1989; Hassell *et al.*, 1991; Comins *et al.*, 1992; Allen *et al.*, 1993; Pascual, 1993). Spatial structure has been suggested as an explanation for the observation that chaotic dynamics, as generated by many simple ecological models, is not widely seen in natural systems. Another important recent result is that local diffusive coupling can often stabilize a collection of unstable populations (Hassell *et al.*, 1991) whereas random global dispersion either has no effect on stability, or a detrimental one (Allen, 1975; Crowley, 1981; Reeve, 1988). The diffusive coupling can give rise to spatial patterns such as spiral waves (as seen in reaction diffusion systems such as the Belousov Zhabotinskii reaction) or static “crystal lattices” as well as spatial chaos.

In this paper I consider the simplest possible model to include spatial effects, namely two coupled logistic maps. This two-dimensional system exhibits a much wider range of dynamic behaviour than the single logistic map, but is still simple enough to allow its

dynamics to be thoroughly studied. I show that coupling chaotic maps can lead to stable, non-chaotic behaviour and that coupling two maps which show periodic behaviour can lead to quasiperiodicity. For large areas of parameter space multiple attractors exist, i.e. the *qualitative* behaviour of the system depends on the initial conditions. This final result has important consequences for the population dynamics as well as providing an important lesson for the modeller of such systems.

### 2. The Model

Consider the simplest biologically realistic model that incorporates spatial effects, two coupled logistic maps (Hastings, 1993; Gyllenberg *et al.*, 1993). In terms of non-dimensional variables, this has the form

$$\begin{aligned}x_{n+1} &= (1-\alpha)f(x_n) + \alpha f(y_n) \\y_{n+1} &= (1-\alpha)f(y_n) + \alpha f(x_n),\end{aligned}\quad (1)$$

where

$$f(x) = \mu x(1-x).$$

This model supposes that the environment consists of two patches between which the individuals diffuse. We assume that there is a density-dependent phase followed by a dispersal phase. The density-dependent phase is modelled by the logistic map, and the dispersal phase by a simple exchange of a fixed proportion of the populations. The parameter  $\mu$  is the standard bifurcation parameter for the logistic map (May, 1976) and  $\alpha$  is a measure of the diffusion of individuals between the two patches, with  $0 \leq \alpha \leq 0.5$ . We assume that the environment is homogeneous, hence the bifurcation parameter  $\mu$  is the same for both patches. The model is similar in spirit to that of Hassell *et al.* (1991), whose host-parasitoid model consists of a pair of variables at each of at least 900 lattice sites. The dynamics of this simpler two-dimensional, two-parameter system will be much easier to understand, and the insights gained by studying it should shed light on the more complex systems.

There are mathematically simpler ways to couple two logistic maps: for instance we could have linear coupling:

$$\begin{aligned} x_{n+1} &= f(x_n) + \alpha(y_n - x_n) \\ y_{n+1} &= f(y_n) + \alpha(x_n - y_n). \end{aligned} \quad (2)$$

Another popular form of coupling is a bilinear coupling, with the linear terms in (2) replaced by  $\pm \alpha x_n y_n$  terms. These forms of the coupled logistic map have been studied previously using both numerical (for instance Kaneko, 1983; Hogg & Huberman, 1984; Ferretti & Rahman, 1988; Satoh & Aihara, 1990*a, b*) and analytic techniques (for instance Sakaguchi & Tomita, 1987). Such forms for the coupling are not biologically realistic as they involve mixing of generations. Some of the individuals have been allowed to reproduce and die and have also been allowed to move into the other patch. We have examined the effects that the different couplings have and we discuss these below.

The behaviour of a single logistic map is well understood, so the method we use to look at the coupled maps is to fix  $\mu$  and vary  $\alpha$ . In this way we can study the effect of coupling maps whose individual behaviour is known. First we choose a  $\mu$  value for which the logistic map has a period  $2^n$  orbit ( $n = 0, 1, 2, \dots$ ). We then investigate the coupled system using analytic and numerical techniques, taking due care when chaos is present. For many dynamical systems the iterates of an initial point are seen to move towards an attracting set (possibly one of many such

sets). Most of the interesting dynamics occur on these attractors and so the behaviour of the system (after the initial transient period) can be discussed in terms of the dynamics of these sets.

The Lyapunov exponents  $\lambda_1$  and  $\lambda_2$  (Schuster, 1989) can be used to distinguish between chaotic, quasiperiodic, periodic and fixed point behaviour. These two exponents measure the long-term average rates of divergence or convergence of nearby orbits in this two dimensional system. We order them so that  $\lambda_1$  is larger. If  $\lambda_1$  is positive then nearby orbits diverge, there is sensitive dependence on initial conditions and hence chaos. If  $\lambda_1$  is zero the motion is quasiperiodic and the attractor is a torus, in our system this means a closed curve, and the orbit never closes. (If the orbit closes after a finite number of iterations, the attractor would be a finite set of points on the torus, and would therefore be a periodic orbit.) If  $\lambda_1$  is negative then we have a periodic orbit, a fixed point being a particular example of this. Notice that the interpretation of the dominant Lyapunov exponent is slightly different when a system is continuous in time (see e.g. Pascual, 1993).

These exponents are calculated as the average of the logarithms of the eigenvalues of the product Jacobian matrix of the map. (The Jacobian matrix  $Df$  is the two-dimensional derivative.) This is a difficult numerical procedure since the  $n$ -step product matrix (as  $n$  becomes large) has eigenvalues  $\Lambda_1^n$  and  $\Lambda_2^n$ , often with  $0 < |\Lambda_2| < 1 < |\Lambda_1|$ . To overcome these problems we use a QR algorithm (Eckmann & Ruelle, 1985) which decomposes the product matrix into a series of better behaved matrices. In the special case of an in-phase attractor ( $x_n = y_n$  for all  $n$ ) it is easy to show that the eigenvalues of the product Jacobian for the coupled map are given by multiplying the derivative of the  $n$ -th iterate of the uncoupled map by 1 or  $(1 - 2\alpha)^n$ . As a result, one Lyapunov exponent is the same as that of the logistic map at the same  $\mu$  value (regardless of  $\alpha$ ) and the other is given by adding  $\log(1 - 2\alpha)$ . This means that if the single logistic map has a stable period  $n$  attractor, then the coupled map will have a stable in-phase period  $n$  attractor for all  $\alpha$ . If the single logistic map has a chaotic attractor, then for  $\alpha$  close enough to 0.5, the second Lyapunov exponent will be negative and an attractor will exist with  $x$  and  $y$  in phase and behaving like a single logistic map at the same  $\mu$  value. The global stability of the in-phase solution is considered by Gyllenberg *et al.* (1993), who prove that the in-phase solution attracts almost all initial conditions when  $\mu$  and  $\alpha$  lie in certain regions of parameter space.

### 3. Results

The single logistic map is a one-dimensional unimodal map and as a result its dynamics are quite limited (Devaney, 1989, discusses these in some detail). In the logistic map only two routes to chaos are observed (period doubling and intermittency), the second dimension allows the quasiperiodic route to occur. Quasiperiodic behaviour occurs when additional frequencies are added to the motion by means of Hopf bifurcations (see Appendix).

The single logistic map can only have one attracting periodic orbit, but multiple attractors are seen in our system, and it is quite easy to understand their existence. Consider the trivial case where  $\alpha=0$  and take (for instance) a  $\mu$  value for which the logistic map has an attracting period  $n$  orbit. We have  $n$  points  $\{p_1, p_2, p_3, \dots, p_n\}$  in the orbit for the logistic map. If we set  $x_0$  to be equal to  $p_i$  (for  $i$  between 1 and  $n$ ) and  $y_0$  equal to  $p_j$  then in our coupled system  $(x_n, y_n)$  will undergo period  $n$  oscillations, but if  $i$  and  $j$  are different there will be a phase difference between  $x_n$  and  $y_n$ . There are  $n$  such phase differences (including the trivial case  $i=j$ ), and so  $n$  distinct attractors will be seen. One attractor will be located on the diagonal  $x=y$  and corresponds to  $i=j$ . If  $(\mu, \alpha)$  is not a bifurcation point, then we can change the parameter values slightly without affecting the behaviour of the system. We have thus demonstrated the existence of multiple attractors for small positive  $\alpha$  (a non-trivial coupling). For some parameter values the difference in dynamics of the attractors is more than just a phase difference, for instance we demonstrate the coexistence of attractors of different periods and the coexistence of chaotic and periodic attractors.

The symmetry of the governing equations implies that if  $\{(x_n, y_n), n \geq 0\}$  is an orbit then  $\{(y_n, x_n), n \geq 0\}$  will also be one. If these two sets are the same then the orbit is symmetric about the diagonal, otherwise the orbit is not symmetric but there is another orbit which is its mirror image. Hence the non-diagonal attractors will either be symmetric about this line or will come in symmetric pairs.

One way of summarizing the behaviour of a system like (1) or (2) is to make a two-dimensional bifurcation diagram (Satoh & Aihara, 1990a, b) consisting of a grid of points in the  $(\mu, \alpha)$  plane which we set to different colours according to the behaviour seen at each pair of parameter values. Such diagrams exhibit beautiful fractal structure and self-similarity. However, the behaviour of the system not only depends on the two parameters but also on the co-ordinates of the initial point, so these diagrams really should be four-dimensional as the set  $(\mu, \alpha, x_0, y_0)$  is needed

to specify the behaviour. This point is acknowledged by Satoh and Aihara, who claim that taking multiple attractors into account does not change the broad structure of the bifurcation diagram, just the fine detail. Since the presentation of the full four-dimensional bifurcation diagram is not easy, this compromise seems well worth making.

In order to study the various attractors as fully as possible, we adopt two strategies. The first is to use many different initial conditions for a given  $\alpha$  and  $\mu$ : these are usually chosen at random. All of the attractors should be seen if enough initial points are chosen. However, if we are near to an  $\alpha$  value where an attractor is created or destroyed (call this  $\alpha_0$ ), only a small set of initial conditions may tend to the attractor in which we are interested. In this case, we choose an initial condition which tends to the attractor when  $\alpha$  is away from  $\alpha_0$ , and change  $\alpha$  slowly towards  $\alpha_0$ . Each time  $\alpha$  is changed, we take the initial condition to be a point on the attractor for the previous  $\alpha$  value. However, we must always be aware that it is possible for attractors to be created and destroyed during small changes in parameter values, and for attractors to have very small basins of attraction. For these reasons it is very easy to miss a lot of behaviour in a numerical study.

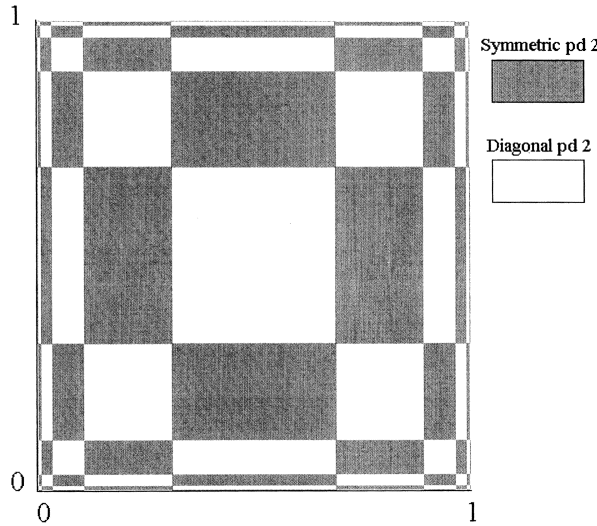
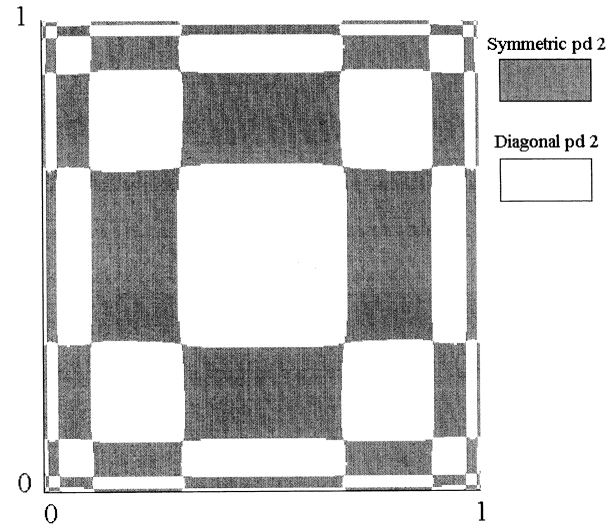
#### 3.1. $\mu = 2.9$

For this parameter value, the logistic map has two fixed points, one stable ( $x^* = (\mu - 1)/\mu$ ) and one unstable ( $\mu = 0$ ). For all  $\alpha$  values almost all points are attracted to  $(x^*, x^*)$ ; both populations tend to the stable fixed point of the uncoupled logistic map. The long-term behaviour of the system for this  $\mu$  value is independent of the strength of the coupling.

#### 3.2. $\mu = 3.2$

For this parameter value, the logistic map has a stable period-2 orbit and two unstable fixed points. For  $\alpha = 0$ , both  $x$  and  $y$  perform period-2 oscillations and the coupled map has two attractors. One lies on the diagonal  $x = y$ , i.e. the two oscillations are in phase. The other attractor is symmetric about the diagonal, the two oscillations are out of phase (in anti-phase). Figure 1 shows the basins of attraction for these two attractors, the figure was produced by iterating  $400 \times 400$  initial points in the unit square and colouring the point according to the asymptotic behaviour of the iterates (see also Hastings, 1993, and Gyllenberg *et al.*, 1993).

The structure of this diagram is easily understood in terms of the uncoupled logistic map,

FIG. 1. Basins of attraction for  $\mu=3.2, \alpha=0$ .FIG. 3. Basins of attraction for  $\mu=3.2, \alpha=0.01$ .

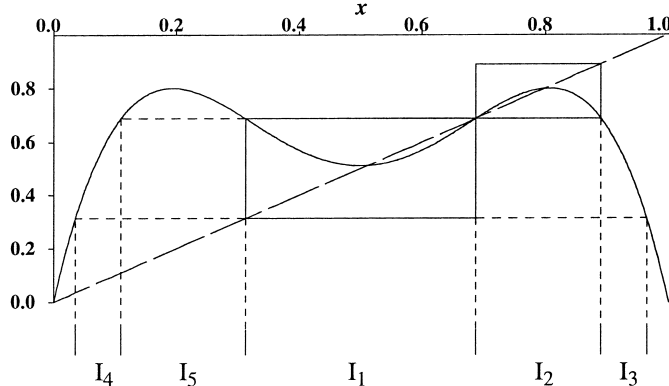
$f(x)=\mu x(1-x)$ . For an initial point  $(x_0, y_0)$ , one needs to know which points in the period two attractor  $x_0$  and  $y_0$  tend to for even (or odd) iterations. In other words, to which of the two stable fixed points of  $f^2$  do  $x_0$  and  $y_0$  tend?

Figure 2 shows the construction of the basins of attraction of  $f^2(x)$ . The interval  $I_1$  is invariant under  $f^2$  and all points in its interior are attracted to the stable fixed point inside  $I_1$ , similarly the interval  $I_2$  is invariant and all points in its interior are attracted to its stable fixed point. The intervals  $I_3$  and  $I_4$  map onto  $I_1$  under  $f^2$ , and interval  $I_5$  maps onto  $I_2$ . We can continue this process, decomposing the unit interval into a collection of open intervals. Points on the boundaries of the intervals get mapped to the unstable fixed point.

Thus when we “couple” two such maps with  $\alpha=0$ , the basins of attraction are open rectangles formed by a cross product of the basins of attraction of the uncoupled maps. For small couplings, this picture

essentially does not change. Figure 3 shows the basins of attraction for  $\alpha=0.01$ , and is topologically equivalent to Fig. 1. As  $\alpha$  increases, the basin of attraction of the in phase solution grows and that of the out of phase solution shrinks.

As we increase  $\alpha$ , the in phase solution remains stable but the out-of-phase solution loses its stability near  $\alpha=0.058$ . This change occurs by a pitchfork bifurcation (Schuster, 1989) of the second iterate of the coupled map, as two unstable points collide with a stable point leaving a single unstable point. Figure 4 shows the basins of attraction just before this bifurcation occurs. As  $\alpha$  approaches the bifurcation point, the basin of the out-of-phase solution shrinks to a set of curves, as the in-phase solution becomes globally stable. Both Hastings (1993) and Gyllenberg *et al.* (1993) examine the existence and stability of period-2 solutions of the map. The latter paper gives analytic expressions for regions of

FIG. 2. Graph of  $f^2(x)$  (solid curve) showing decomposition of  $[0, 1]$  into open intervals that map to one of the stable fixed points of  $f^2$  under iteration of  $f^2$ .

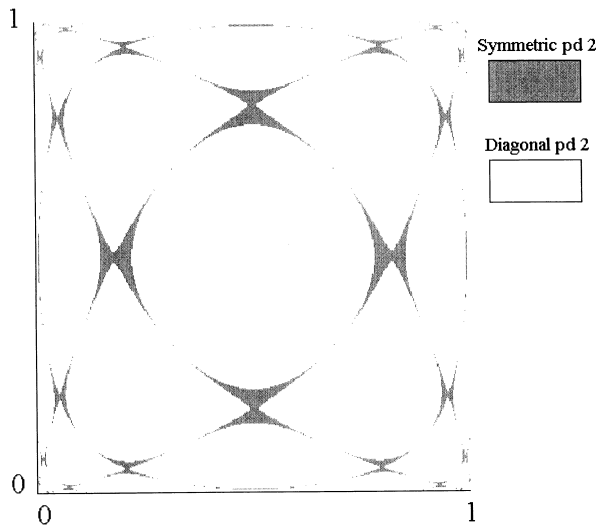


FIG. 4. Basins of attraction for  $\mu=3.2$ ,  $\alpha=0.058$ , just before the symmetric period-2 orbit loses stability.

parameter space within which the in-phase and out-of-phase period-2 solutions are stable, which provided a check for some of our numerical results.

### 3.3. $\mu=3.5$

For this parameter value, the logistic map has a stable period-4 orbit, an unstable period-2 orbit, and two unstable fixed points. For  $\alpha=0$  there are four period-4 attractors, corresponding to  $x$  and  $y$  undergoing period-4 oscillations with four phase differences. The in phase attractor lies on the diagonal and the anti-phase ( $x_n=y_{n+2}$ ) attractor is symmetric about the diagonal. The two remaining attractors are asymmetric, with one being the mirror image of the other. The four attractors are shown in Fig. 5 and their basins of attraction in Fig. 6. The structure of the basins of attraction is explained in the same way as for the  $\mu=3.2$  case, except that one looks at  $f^4$  instead of  $f^2$ .

As  $\alpha$  is increased past about 0.0123, quasiperiodic behaviour is observed as the two asymmetric period-4 orbits give way to a single attractor consisting of two tori (Fig. 7). These stable period-4 points are

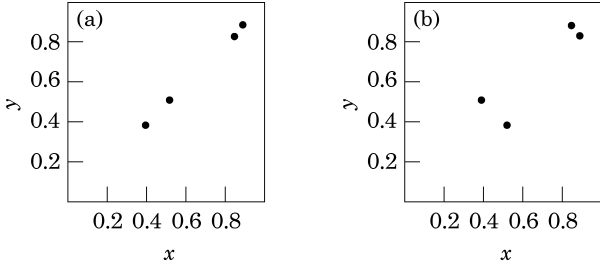


FIG. 5. The four period-4 attractors seen for  $\mu=3.5$ ,  $\alpha=0$ . (a) In phase (diagonal), (b) symmetric, (c) and (d) pair of asymmetric orbits.

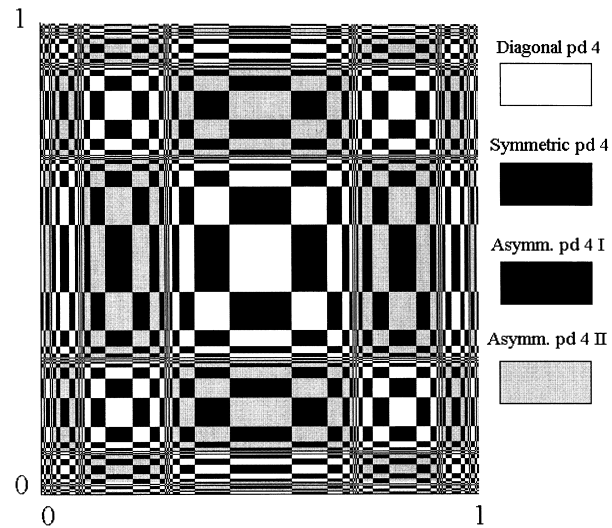
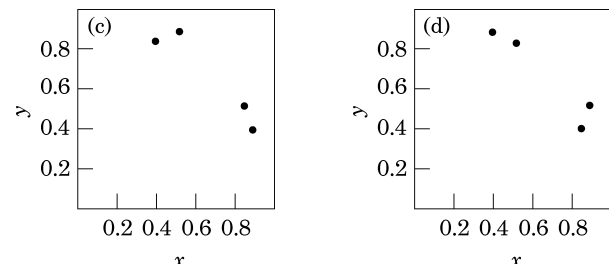


FIG. 6. Basins of attraction for  $\mu=3.5$ ,  $\alpha=0$ .

destroyed in saddle-node bifurcations (Devaney, 1989) as they collide with nearby unstable period-4 points. This quasiperiodic attractor then undergoes a reverse Hopf bifurcation when  $\alpha$  is just below 0.0171, leaving a stable period-2 orbit. The symmetric period-4 orbit loses stability when  $\alpha$  is just below 0.0364, in a pitchfork bifurcation. The period-2 orbit loses stability by a pitchfork bifurcation for  $\alpha$  just above 0.122, leaving the in-phase (diagonal) period-4 solution globally stable. Figure 8 is a plot of the largest Lyapunov exponent for each attractor seen as  $\alpha$  increases from 0 to 0.15. The region for which quasiperiodic behaviour occurs is clearly seen as a range of  $\alpha$  values for which this exponent is zero. Figure 9 shows the basins of attraction seen for various  $\alpha$  values.

We can continue in this fashion, coupling maps with period  $2^n$  orbits; we see  $2^n$  attractors for  $\alpha$  near 0 and these attractors undergo bifurcations in a very similar way to those previously described. In no case have we observed chaotic behaviour arising as a consequence of coupling such stable single maps. (Although, one must remember the warning given before about the possibility that the dynamics may change over small



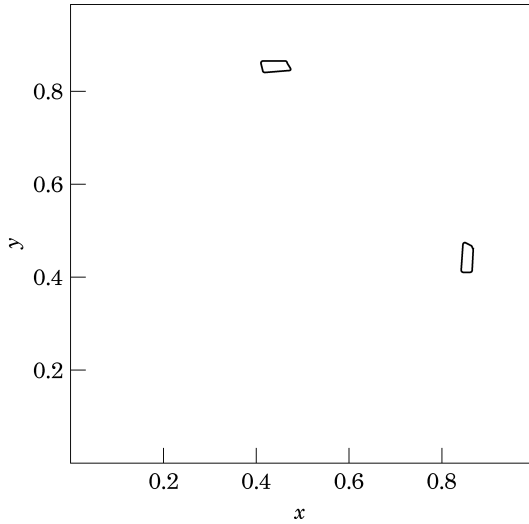


FIG. 7. Two-torus attractor seen for  $\mu = 3.5$ ,  $\alpha = 0.015$ .

intervals of parameters or that attractors may be created with very small basins of attraction.)

We now turn our attention to the situation when the individual maps are chaotic. We couple maps whose chaotic attractors have  $2^n$  band structure, that is the attractor is contained within  $2^n$  sub-intervals of  $[0, 1]$  which are invariant under  $f^{2^n}$  and are permuted by  $f$ .

#### 3.4. $\mu = 3.7$

The logistic map exhibits one band chaos for this parameter value. When the maps are coupled with  $\alpha = 0$  we see just one attractor, which is square and symmetric about the diagonal. As the coupling

is increased the attractor undergoes a complicated sequence of changes. Many intervals of  $\alpha$  values give periodic behaviour, as is seen in the single logistic map beyond the onset of chaos. As a result of this, a numerical study of the system will tend to miss a lot of periodic behaviour. Before discussing these periodic windows, we consider the main changes that the chaotic attractor undergoes as the coupling is increased.

As  $\alpha$  is increased between 0.0130 and 0.0135, the single block chaotic attractor suddenly changes into a two block attractor. A qualitative change in the structure of the chaotic attractors has occurred, such a change is known as a *crisis*. This type of crisis is called an interior crisis (Grebogi *et al.*, 1982, 1983; Sakaguchi & Tomita, 1987), and it is most easily understood by considering the attractors changing with decreasing  $\alpha$ . As  $\alpha$  decreases, the two blocks of the attractor grow and move closer together. At the crisis, the blocks collide with an unstable fixed point on the basin boundary (in this case the unstable point is  $(x^*, x^*)$ , on the diagonal). Points which come near enough to the unstable point are then thrown out into the new part of the attractor. The point then wanders around the new part of the attractor for a while before returning to the part of the attractor which existed before. As a result, in the neighbourhood of the crisis very long intermittent behaviour is observed, with the point wandering around the two parts of the chaotic set for periods of time with sudden jumps between the two. Figure 10 shows the chaotic attractors in the vicinity of the crisis.

As  $\alpha$  is increased between 0.041 and 0.042, we observe another crisis. The symmetric two-block

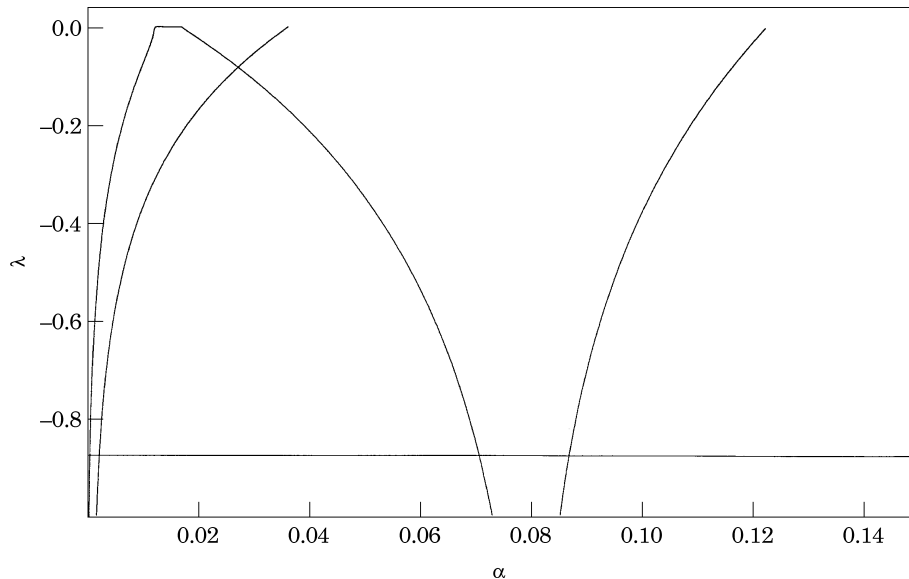


FIG. 8. Plot of largest Lyapunov exponent ( $\lambda$ ) vs  $\alpha$  for each of the attractors seen for  $\mu = 3.5$ . Quasiperiodic behaviour is seen when  $\lambda = 0$ . The pitchfork bifurcations are seen to occur as  $\lambda$  becomes zero and the curves end.

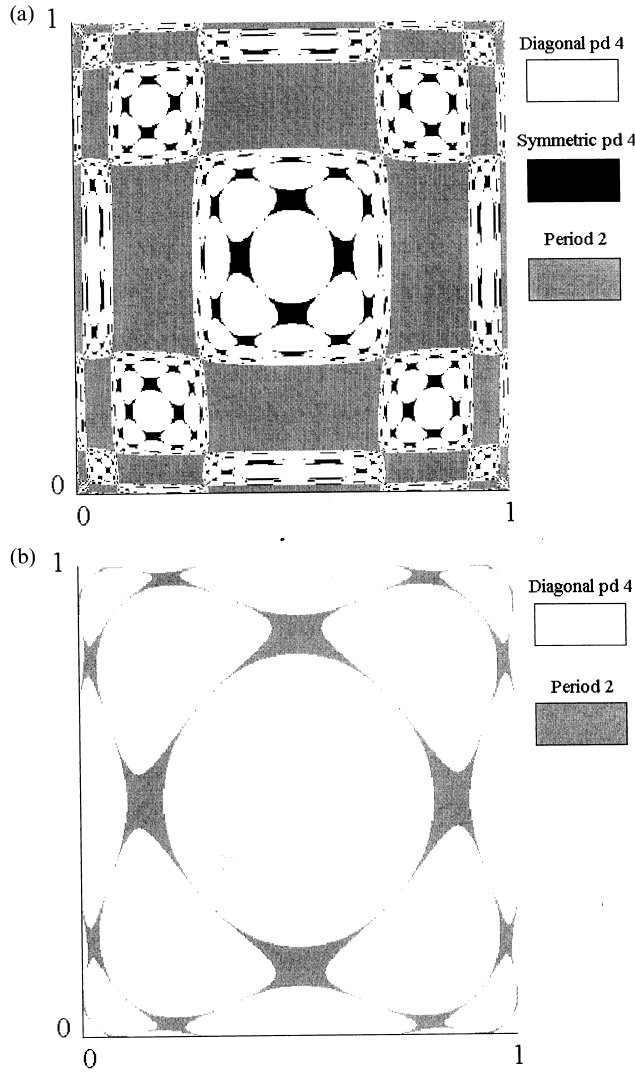


FIG. 9. Basins of attraction for  $\mu = 3.5$ . (a)  $\alpha = 0.035$ , just before the symmetric period-4 orbit is lost. (b)  $\alpha = 0.12$ , just before the period-2 orbit becomes unstable.

attractor splits into a pair of asymmetric four piece attractors. This is known as an attractor merging crisis (Ott, 1993). Intermittent behaviour is again observed just before the crisis (for example at  $\alpha = 0.0419$ ) with iterates behaving almost as if there were two separate attractors. The iterates are seen to move around one-half of the attractor before being thrown onto the other half, where they move around for a while before returning to the first half.

A cascade of crises occurs as  $\alpha$  is increased further, resulting in a pair of asymmetric period  $2^n$  piece chaotic attractors being seen. (For instance, eight pieces are seen when  $\alpha = 0.048$ , 16 when  $\alpha = 0.0484$ .) These crises accumulate just below 0.0486, which is also the accumulation point of a cascade of reverse period doublings which then follows. Periodic orbits of

periods  $2^n$  are seen for  $n \geq 2$ , the final result of this cascade being a pair of asymmetric period-4 orbits. These orbits can be seen, for instance, when  $\alpha = 0.056$ .

These period-4 orbits are destroyed in saddle node bifurcations just below  $\alpha = 0.05614$ . The attractor formed appears to be made up of two tori which are very wavy near to where the periodic points used to be. Such an attractor has been observed in other studies of coupled maps (Hogg & Huberman, 1984; Kaneko, 1984), and its structure is studied in detail by Kaneko (1984). The motion on this attractor appears to be chaotic just above the bifurcation point (although this chaos is punctuated by periodic windows). As the coupling is increased, the waves become straightened and the motion becomes quasiperiodic (Fig. 11.). This attractor undergoes a reverse Hopf bifurcation when  $\alpha$  is between 0.0746 and 0.0747, giving rise to a period-2 orbit. The orbit becomes unstable just below 0.155 in a pitchfork bifurcation. These last two bifurcations, involving period-2 orbits, occur just as predicted by the analytic results of Gyllenberg *et al.* (1993).

One example of a periodic window occurs when  $0.0413 < \alpha < 0.0418$ , when a period-12 window is seen. The window begins as a crisis turns the symmetric two-block chaotic attractor into a pair of asymmetric 12-piece attractors. These attractors undergo a cascade of further crises giving rise to 24, 48, and 96 pieces, and so on. These crises accumulate at a certain  $\alpha$  value, which is the accumulation of a reverse period-doubling cascade that follows. This cascade ends with a pair of asymmetric period-12 orbits. Towards the end of the window, long chaotic transients are seen before the system settles down to periodic behaviour. The periodic behaviour ends as the two stable period-12 orbits collide with and destroy two unstable period-12 orbits in two simultaneous saddle node bifurcations. A bifurcation diagram for one of the attractors during the window is shown in Fig. 12. (We plot 20000  $x_n$  values for each  $\alpha$  value, after allowing transients to die out. When these are plotted on a scale from 0 to 1, they are seen to cluster around 12  $x$  values. Figure 12 is a magnification of one of these clusters. The initial condition is chosen so that the same attractor of the pair is explored each time.) Notice the self-similarity that is seen in this system; the bifurcation structure within the window is very similar to the main bifurcation sequence described above with crises and reverse period doublings. Within the figure, we see periodic windows which follow bifurcation sequences similar to that of the whole figure. Just beyond the end of the periodic window we observe intermittent behaviour (Schuster, 1989). The iterates move very slowly when they come near to where the fixed points

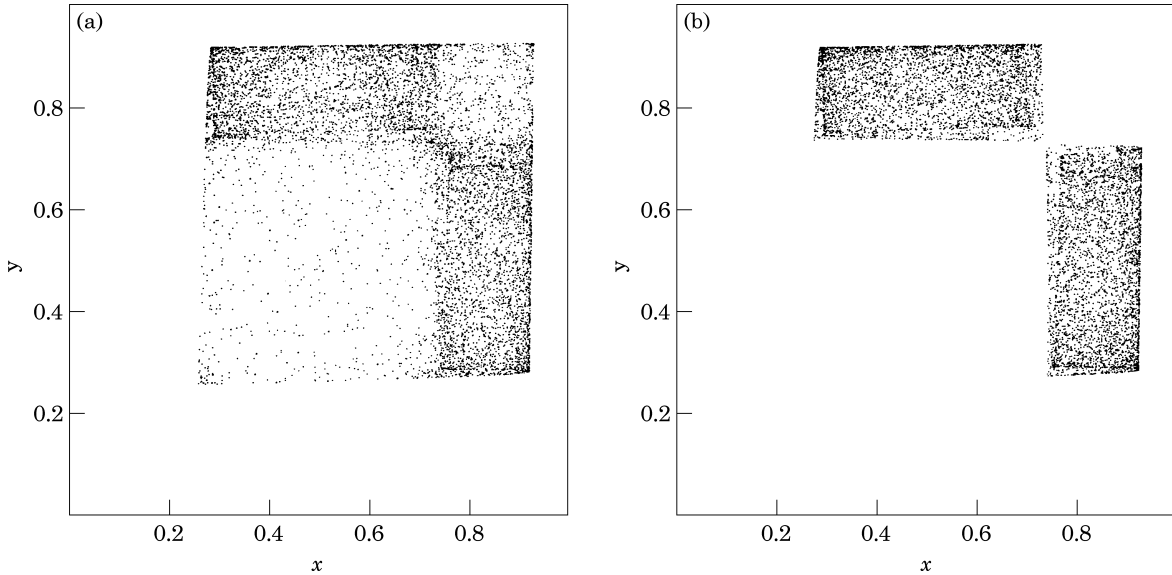


FIG. 10. Chaotic attractors in vicinity of the crisis,  $\mu = 3.7$ . (a) Diagonal block attractor seen for  $\alpha = 0.012$ . (b) Symmetric two-block attractor seen for  $\alpha = 0.0135$ .

used to be, and during these episodes the dynamics are nearly periodic. Once the iterate has left this region the motion becomes chaotic until the iterate comes close to the region again. Over a long period of time we observe nearly periodic dynamics punctuated by episodes of chaotic behaviour.

For some  $\alpha$  values within this bifurcation sequence we see the creation of new attractors. For instance, just above 0.0913 we see the creation of a chaotic attractor. This attractor then undergoes various bifurcations going from chaos to torus to a period-4 orbit, with various periodic orbits interrupting this sequence. The period-4 orbit disappears just below 0.1269 in a pitchfork bifurcation. This process is repeated in the interval (0.1012, 0.1037). Figure 13 shows the basins of attraction of the various attractors seen when  $\alpha = 0.1018$ . (Points that start on the diagonal will remain on the diagonal, undergoing chaotic

dynamics, even though the in phase set is not attracting in this case. We do not show this behaviour on the basins of attraction plot since there are points arbitrarily close which tend to one of the attracting sets.)

For large values of the coupling, the only attracting set is an in-phase chaotic attractor, with both  $x$  and  $y$  behaving as a single logistic map with  $\mu = 3.7$ . The in-phase chaotic set becomes an attractor as its smaller Lyapunov exponent becomes negative when  $\alpha$  is between 0.149 and 0.150. Below this  $\alpha$  value a symmetric chaotic set is seen, although this may be very long transient behaviour. For some  $\alpha$  values below 0.149 the in-phase set appears to be an attractor even though the smaller Lyapunov exponent is positive, corresponding to points of the diagonal moving away exponentially on average. We believe this is a numerical effect caused by the finite precision of the

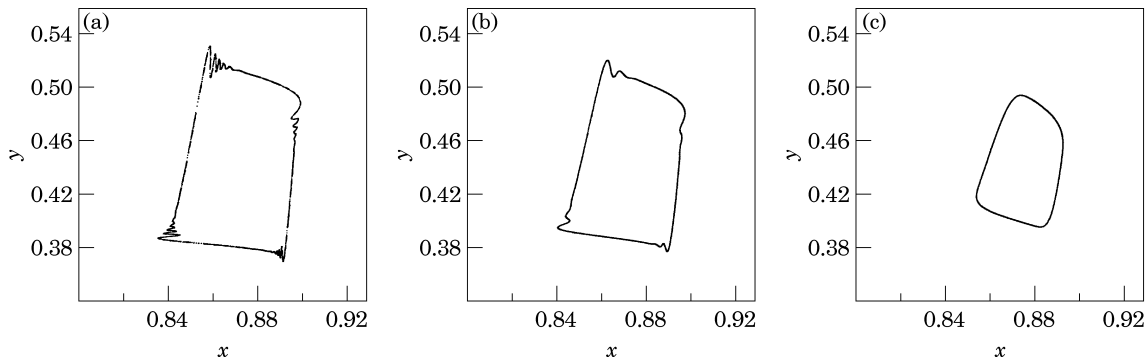


FIG. 11. Magnification of one of the two tori seen for  $\mu = 3.7$ . (a) Wavy tori,  $\alpha = 0.0574$ . (b)  $\alpha = 0.604$ , notice the torus is less wavy (c)  $\alpha = 0.674$ , when the tori have lost the waves.

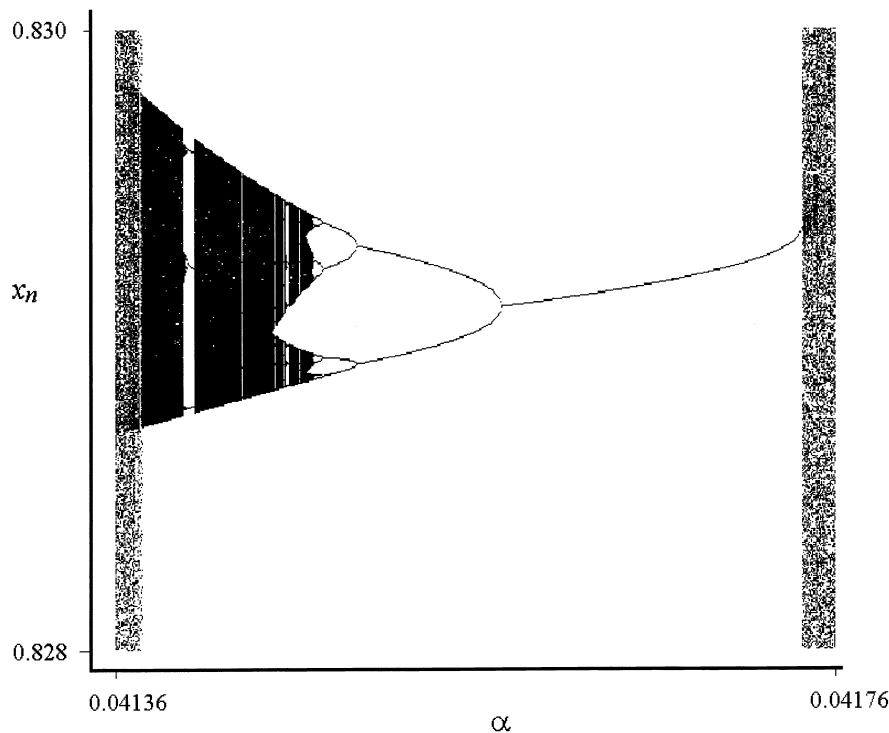


FIG. 12. Bifurcation structure observed during a periodic window when  $\mu=3.7$ . This figure is a magnification about one of the 12 clusters of  $x_n$  values seen. At the extreme left of the figure we see the crisis which gives rise to the window. A cascade of reverse crises follows, interrupted by further periodic windows. Further right, a reverse period-doubling cascade can be seen. The window ends with a saddle node bifurcation at the right of the figure.

computer arithmetic. If the iterate  $(x_n, y_n)$  comes close enough to the diagonal then the computer may set  $x_n = y_n$  and all future iterates will then stay on the diagonal. After the loss of the stable period two orbit near 0.155, almost all initial conditions are attracted to the in-phase chaotic attractor.

### 3.5. $\mu=3.65$

The individual maps show two-band chaos, for no coupling we see two attractors; one consists of two square blocks centred on the diagonal, and the other is a symmetric pair of rectangular blocks. As the coupling is increased, both of these attractors undergo bifurcation sequences which are extremely similar to that seen in the  $\mu=3.7$  case. For this reason we shall not give as much detail in describing these sequences, instead we shall give an  $\alpha$  value when each different attractor described can be seen. (We do not give the  $\alpha$  values of the bifurcation points.)

The symmetric two-block attractor undergoes a crisis, giving rise to a pair of asymmetric four-block chaotic attractors (these new attractors can be seen, for instance, when  $\alpha=0.025$ ). Later, these attractors undergo a cascade of crises followed by a reverse period-doubling cascade which ends up with a pair

of asymmetric period-4 orbits ( $\alpha=0.042$ ). These are destroyed in saddle node bifurcations, leaving a two-torus attractor with quasiperiodic dynamics ( $\alpha=0.047$ ). In this case we do not see chaotic behaviour between the loss of the periodic orbits and the quasiperiodic behaviour (although it could

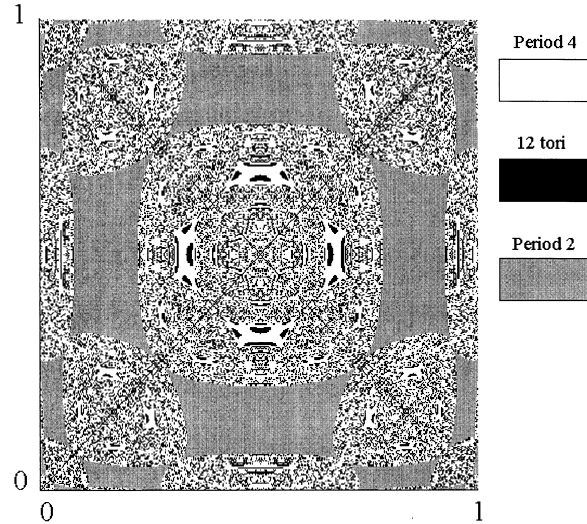


FIG. 13. Basins of attraction for  $\mu=3.7$ ,  $\alpha=0.1018$ . Notice the particularly detailed self-similar structure.

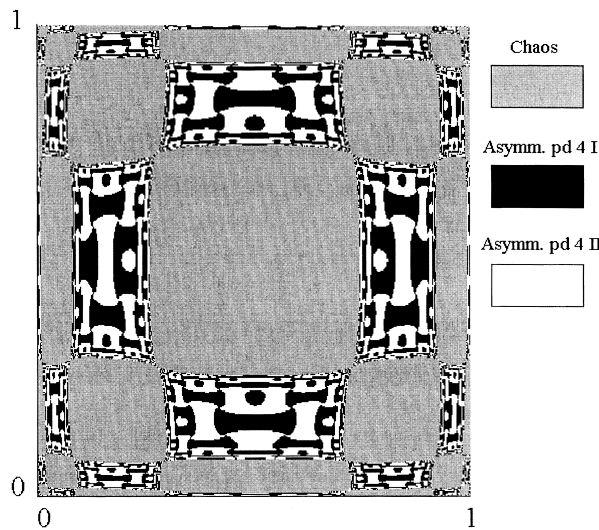


FIG. 14. Basins of attraction for  $\mu=3.65$ ,  $\alpha=0.045$ .

occur over a very small parameter range). A reverse Hopf bifurcation causes the attractor to become a period-2 orbit ( $\alpha=0.06$ ). This orbit loses stability in a pitchfork bifurcation near 0.147.

The “diagonal” two block attractor undergoes a similar bifurcation sequence. The attractor becomes a symmetric four-block attractor in a crisis ( $\alpha=0.057$ ). A complicated bifurcation sequence follows which results in a quasiperiodic four-torus attractor being seen ( $\alpha=0.07$ ). Later this becomes a symmetric period-4 orbit in a reverse Hopf bifurcation ( $\alpha=0.075$ ). The period-4 orbit finally loses stability in a pitchfork bifurcation when  $\alpha$  is near 0.109. Once again, periodic windows are seen within this bifurcation sequence.

Periodic windows are seen throughout the chaotic parameter regions. For instance, we see that the symmetric four-piece attractor has a large periodic window within the interval (0.062, 0.064). Within this window, in addition to period doublings and crises, we see the multiple Hopf bifurcations characteristic of the quasiperiodic route to chaos (see Appendix). For  $\alpha=0.06248$ , we see a period-44 ( $=4 \times 11$ ) orbit, and as we decrease  $\alpha$  a Hopf bifurcation occurs leaving 44 tori (for instance when  $\alpha=0.0624$ ). As  $\alpha$  is decreased further we see a period-308 ( $=44 \times 7$ ) orbit ( $\alpha=0.06212$ ) which undergoes a further Hopf bifurcation, giving rise to a 308-torus attractor ( $\alpha=0.06209$ ). As  $\alpha$  is decreased further, the tori break up and the dynamics become chaotic.

Figure 14 shows the basins of attraction seen for  $\alpha=0.045$ , when the chaotic attractor which is the product of the diagonal two-block coexists with a pair

of asymmetric period-4 orbits which resulted from the symmetric two-block attractor.

As in the  $\mu=3.7$  case, attractors are created which undergo similar bifurcation sequences before being destroyed. One example of this occurs within the interval (0.070, 0.073). Figure 15 shows the basins of attraction for  $\alpha=0.070875$ , when a period-2 orbit (the product of the symmetric two block), a four-torus attractor (the product of the diagonal two block) and a period-36 orbit (a product of the new attractor) coexist.

For large values of the coupling, the only attracting set is an in-phase chaotic attractor, with both  $x$  and  $y$  behaving as a single logistic map with  $\mu=3.65$ . The second Lyapunov exponent of the in phase set becomes negative when  $\alpha$  is near 0.113. After the loss of the stable period two orbit near 0.147, almost all initial conditions are attracted to the in-phase chaotic attractor.

We have repeated these calculations for other  $\mu$  values for which the logistic map shows  $2^n$  band chaos. Similar bifurcation sequences are observed, with chaos going to quasiperiodicity, then to periodic behaviour. The in phase attractor is always favoured by large values of the coupling, with both  $x$  and  $y$  behaving like iterates of the single logistic map at the same  $\mu$  value.

#### 4. The Effects of Linear Coupling

In this section we discuss how the results seen above are changed if we employ a linear coupling, as in eqns (2). This form of coupling may be considered as a discrete space analogue of the Laplacian ( $\nabla^2$ ) coupling used in reaction-diffusion equations. The linear

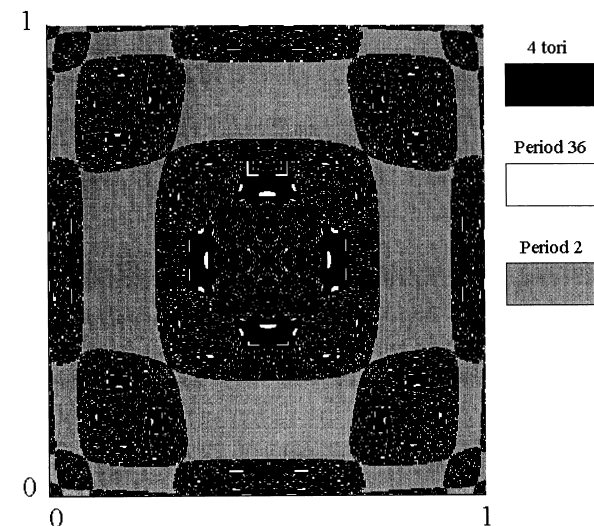


FIG. 15. Basins of attraction for  $\mu=3.65$ ,  $\alpha=0.070875$ .

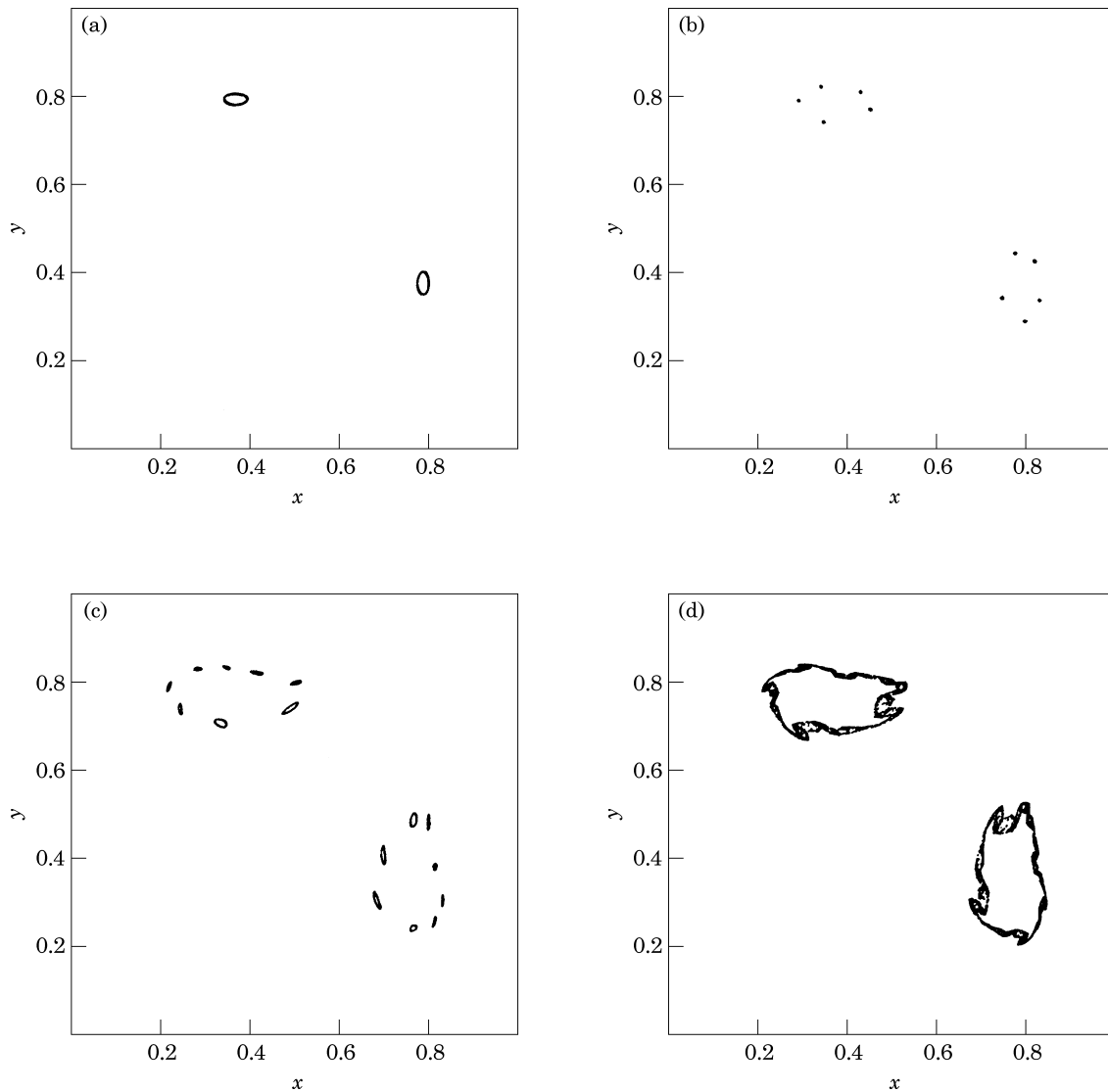


FIG. 16. Structure of attractors for  $\mu=2.9$  with linear coupling. (a) Two tori,  $\alpha=0.27$ ; (b) frequency locking (period 10),  $\alpha=0.29$ ; (c) one of the asymmetric pair of 16 tori,  $\alpha=0.326$ ; (d) chaos,  $\alpha=0.3314$ .

coupling is also mathematically convenient as it does not introduce any extra nonlinear terms into the equations. The coupling is not biologically realistic, however, and it does cause some unexpected behaviour to occur.

One example of this unexpected behaviour occurs when we couple two logistic maps with  $\mu=2.9$  using linear coupling. For this parameter value, as discussed previously, the logistic map has two fixed points; one stable ( $x^*=(\mu-1)/\mu$ ) and one unstable ( $\mu=0$ ). For  $\alpha \in [0, 0.05]$  almost all points are attracted to  $(x^*, x^*)$ . At  $\alpha=0.05$  this point becomes unstable as it undergoes a period doubling bifurcation, creating a stable period-2 attractor that is symmetric in  $(x, y)$ :  $\{(x_1, y_1), (y_1, x_1)\}$ .

As  $\alpha$  increases further, the period-2 attractor undergoes a Hopf bifurcation (at  $\alpha$  just below 0.268), producing two symmetric tori. These tori undergo a complex sequence of bifurcations, including further frequency lockings and Hopf bifurcations. One example of frequency locking is seen between about 0.289 and 0.298 when a period-10 orbit is seen. An asymmetric pair of period-16 orbits can be seen when  $\alpha=0.325$ ; these undergo Hopf bifurcations, producing an asymmetric pair of 16 tori which can be seen, for instance, when  $\alpha=0.3256$ . Chaotic behaviour is seen as  $\alpha$  is increased, for instance when  $\alpha=0.3314$ . Periodic windows are seen beyond this  $\alpha$  value, as they are in the single logistic map beyond the onset of chaos. Figure 16 shows some of the

attractors seen for this value of  $\mu$  as  $\alpha$  varies. Multiple attractors are seen for this value of  $\mu$ , for example when  $\alpha = 0.325$  a two-torus attractor coexists with the period-16 orbits described above. This is in contrast to the nonlinear coupling of the two maps at this  $\mu$  value, when only one attractor was ever seen.

The coupling is seen to destabilize individually stable maps, producing chaotic behaviour. We also observe that the in-phase attractor is no longer favoured by large couplings. Similar behaviour is observed for other  $\mu$  values for which the logistic map exhibits stable periodic behaviour. This counterintuitive behaviour is purely a consequence of the incorrect coupling of the two maps.

When two chaotic logistic maps are coupled in this fashion, we again see that the coupling can lead to stable behaviour. Bifurcation sequences similar to those described for nonlinear coupling are seen. As for the periodic maps, large coupling no longer favours the in-phase attractor.

The dangers of coupling discrete time maps with linear coupling terms have been noted before. Kot & Schaffer (1986) developed integrodifference equations to model growth and dispersal, and used nonlinear couplings. In their paper they note that linear couplings mix generations and may lead to counterintuitive results. Jackson (1990) considers coupling maps in a more general context, and warns that the diffusive process must be kept separate from the reproductive process in order to keep in touch with “reality”.

## 5. Discussion

The model shows many interesting types of behaviour which may be important when considering the dynamics of real populations. The most important result is that the scale on which measurements of the population is taken is crucial, and that information on the distribution of the population is also necessary to understand the dynamics. A similar result was found by Sugihara *et al.* (1990) when analysing the monthly incidence of measles in England and Wales. On a city-by-city scale they found evidence of low-dimensional chaos, whereas on a country-wide scale the dynamics appeared to be a two-year noisy cycle. Coupling can stabilize individually chaotic subpopulations to give stable dynamics of the population as a whole. The reverse is also seen with quasiperiodic dynamics resulting from the coupling of two populations that individually show identical periodic behaviour.

We may ask what sort of dynamic behaviours are preferable for the population as a whole to persist. It has

been suggested that chaotic behaviour of the population as a whole may increase the probability of extinction because (for many chaotic systems) there is a high probability that the population density will eventually go below an extinction threshold (Berryman & Millstein, 1989). If the population is patchy this would not necessarily be the case, unless the populations in different patches were synchronized. In this system, strong coupling between patches will lead to them being synchronized even if they were individually chaotic. However, if the populations in different patches were not synchronized, then diffusion between patches would be able to counteract local extinctions. Similar results have been seen in simulations where coupling large arrays of chaotic Rössler attractors gave rise to stable spiral patterns which could withstand the obliteration of large parts of the spiral (Klevecz *et al.*, 1991). In weakly coupled systems it has been suggested that chaos can amplify local population noise, leading to a greater degree of asynchrony between local populations (Allen *et al.*, 1993).

The existence of multiple attractors means that populations can exhibit very different dynamic behaviours, even if per capita birth and death rates and diffusion rates are the same. It is possible that a sudden change in the populations due to some external cause can move the system between these different behaviours, in some cases from stable to chaotic dynamics. If an attractor is close to the edge of its basin of attraction then only a small perturbation (for instance small amplitude random noise) may be necessary to switch the system from one sort of behaviour to another.

If the parameters of the model are allowed to vary with time there can be dramatic changes in the population dynamics. The crises and periodic windows that were seen represent dramatic changes in the behaviour for very small changes in the parameters. In the vicinity of these changes, long episodes of intermittent and transient behaviours are seen. Populations may exhibit apparently periodic behaviour for long periods of time and then suddenly undergo chaotic bursts before returning to almost periodic behaviour. This means that if a population is observed over a short period of time then the interesting part of the dynamics may be missed, since for most of the time the dynamics appear tame.

The multiple attractors pose a trap for the unwary numerical experimenter. One method that has been used to study eqns (2) is to fix one initial point and consider iterates for different values of the coupling and bifurcation parameters. Whilst this is fine for the single logistic map (which has just one attracting set), this will not do here. As parameters change so the basins of

attraction grow and shrink, our one initial point may find itself in a different basin and a change in behaviour will be observed. This change in behaviour is due entirely to the multiple attractors and not to some change in the dynamics of the map. Many authors have fallen into this trap; for instance Ferretti & Rahman (1988) studied the map numerically by iterating the single initial condition (0.5, 0.5).

## 6. Conclusions

The coupled logistic map exhibits a much wider range of dynamic behaviour than the single logistic map, much of which may be important to the study of population dynamics. Intermittent behaviour may lead to populations behaving almost periodically for long periods of time but with short bursts of apparently random behaviour. Crisis behaviour may be more dramatic, with sudden changes in dynamic behaviour occurring for small changes in the parameters controlling the nature of the dynamics. The spatial nature of the problem is seen to be important, with the coupling able to cause individually stable periodic populations to undergo quasiperiodic dynamics, or able to stabilize individually chaotic populations. More realistic models would include better descriptions of the local dynamics (although for simple models one tends to see similar types of dynamics) and of the spatial degrees of freedom. The latter would require the consideration of more patches and a more detailed description of movement between patches. Inhomogeneities in the environment could be considered by varying the coupling and bifurcation parameters across the lattice.

This work was supported by the Wellcome Trust (Biomathematical Scholarship, grant number 036134/Z/92/Z). I wish to thank R. M. May for discussions and encouragement. I also wish to thank two anonymous referees whose helpful criticisms and thoughtful comments on the original manuscript led to major improvements in this work.

## REFERENCES

- ALLEN, J. C. (1975). Mathematical models of species interactions in time and space. *Am. Nat.* **109**, 319–342.
- ALLEN, J. C., SCHAFER, W. M. & ROSKO, D. (1993). Chaos reduces species extinction by amplifying local population noise. *Nature, Lond.* **364**, 229–232.
- BERRYMAN, A. A. & MILLSTEIN, J. A. (1989). Are ecological systems chaotic—and if not, why not? *TREE* **4**, 26–28.
- COMINS, H. N., HASSELL, M. P. & MAY, R. M. (1992). The spatial dynamics of host-parasitoid systems. *J. Anim. Ecol.* **61**, 735–748.
- CROWLEY, P. H. (1981). Dispersal and the stability of predator-prey interactions. *Am. Nat.* **118**, 673–701.
- CURRY, J. & YORKE, J. A. (1978). A transition from Hopf bifurcation to chaos: computer experiments with maps in  $\mathbb{R}^2$ . In: *The Structure of Attractors in Dynamical Systems*. Berlin: Springer-Verlag.
- DEVANEY, R. L. (1989). *An Introduction to Chaotic Dynamical Systems*. Redwood City, CA: Addison Wesley.
- ECKMANN, J.-P. & RUELLE, D. (1985). Ergodic theory of chaos and strange attractors. *Rev. Mod. Phys.* **57**, 617–656.
- FERRETTI, A. & RAHMAN, N. K. (1988). A study of coupled logistic map and its applications in chemical physics. *Chem. Phys.* **119**, 275–288.
- GREBOGI, C., OTT, E. & YORKE, J. A. (1982). Chaotic attractors in crisis. *Phys. Rev. Lett.* **48**, 1507–1510.
- GREBOGI, C., OTT, E. & YORKE, J. A. (1983). Crises, sudden changes in chaotic attractors, and transient chaos. *Physica D* **7**, 181–200.
- GYLLENBERG, M., SÖDERBACKA, G. & ERICSSON, S. (1993). Does migration stabilize local population dynamics? Analysis of a discrete metapopulation model. *Math. BioSci.* **118**, 25–49.
- HASSELL, M. P., COMINS, H. N. & MAY, R. M. (1991). Spatial structure and chaos in insect population dynamics. *Nature, Lond.* **353**, 255–258.
- HASTINGS, A. (1993). Complex interactions between dispersal and dynamics: lessons from coupled logistic equations. *Ecology* **74**, 1362–1372.
- HOGG, T. & HUBERMAN, B. A. (1984). Generic behavior of coupled oscillators. *Phys. Rev. A* **29**, 275–281.
- JACKSON, E. A. (1990). *Perspectives of Nonlinear Dynamics*, Vol. 2. Cambridge: Cambridge University Press.
- KANEKO, K. (1983). Transition from torus to chaos accompanied by frequency lockings with symmetry breaking. *Prog. Theor. Phys.* **69**, 1427–1442.
- KANEKO, K. (1984). Oscillation and doubling of torus. *Prog. Theor. Phys.* **72**, 202–215.
- KLEVÉCZ, R. R., PILLIOD, J. & BOLEN, J. (1991). Autogenous formation of spiral waves by coupled chaotic attractors. *Chronobiology Int'l.* **8**, 6–13.
- KOT, M. (1989). Diffusion-driven period-doubling bifurcations. *BioSystems* **22**, 279–287.
- KOT, M. & SCHAFER, W. M. (1986). Discrete-time growth-dispersal models. *Math. BioSci.* **80**, 109–136.
- MAY, R. M. (1976). Simple mathematical models with very complicated dynamics. *Nature, Lond.* **261**, 459–467.
- NEWHOUSE, S., RUELLE, D. & TAKENS, F. (1978). Occurrence of strange axiom-A attractors near quasiperiodic flow on  $T^m$ ,  $m \geq 3$ . *Commun. Math. Phys.* **64**, 35–40.
- OTT, E. (1993). *Chaos in Dynamical Systems*. Cambridge: Cambridge University Press.
- PASCUAL, M. (1993). Diffusion-induced chaos in a spatial predator-prey system. *Proc. R. Soc. Lond. B* **251**, 1–7.
- REEVE, J. D. (1988). Environmental variability, migration and persistence in host-parasitoid systems. *Am. Nat.* **132**, 810–836.
- RUELLE, D. & TAKENS, F. (1971). On the nature of turbulence. *Commun. Math. Phys.* **20**, 167–192.
- SAKAGUCHI, H. & TOMITA, K. (1987). Bifurcations of the coupled logistic map. *Prog. Theor. Phys.* **78**, 305–315.
- SATO, K. & AIHARA, T. (1990a). Numerical study on a coupled-logistic map as a simple model for a predator-prey system. *J. Phys. Soc. Jpn.* **59**, 1184–1198.
- SATO, K. & AIHARA, T. (1990b). Self-similar structures in the phase diagram of a coupled-logistic map. *J. Phys. Soc. Jpn.* **59**, 1123–1126.
- SCHUSTER, H. G. (1989). *Deterministic Chaos, An Introduction*, 2nd revised edn. Weinheim: Physik-Verlag.
- SUGIHARA, G., GRENfell, B. & MAY, R. M. (1990). Distinguishing error from chaos in ecological time series. *Phil. Trans. R. Soc. Lond. B* **330**, 235–251.

## APPENDIX

### The Hopf Bifurcation and Quasiperiodicity

For most sets of parameter values, altering them slightly does not change the qualitative behaviour of the system. The changes in qualitative behaviour are

known as bifurcations and the parameter values at which they occur are called bifurcation points. Some bifurcations only affect the dynamics in a small neighbourhood; these are called local bifurcations. Such bifurcations are associated with one or more of the eigenvalues of the Jacobian matrix  $Df$  having modulus one. (This is for a fixed point; for period  $n$  orbits one considers the product Jacobian  $Df^n$ .) Two simple bifurcations which are observed in our system are saddle node (where a pair of fixed points of  $f^n$  are produced, one stable and one unstable) and period doubling (where a stable period  $n$  orbit loses its stability and a stable period  $2n$  orbit is created), these are both seen in the logistic map. The second dimension allows other bifurcations to occur, including the Hopf bifurcation.

The Hopf bifurcation occurs when a complex conjugate pair of eigenvalues crosses the unit circle (if there is a complex eigenvalue  $a+ib$  then its complex conjugate  $a-ib$  is also an eigenvalue as the Jacobian matrix is real). At this point a fixed point undergoes a change in stability and an invariant curve is created. This is most easily seen in a simple example. Consider the following two-dimensional map

$$F\begin{pmatrix} x \\ y \end{pmatrix} = \{\lambda - (x^2 + y^2)\} \begin{pmatrix} \cos \alpha & -\sin \alpha \\ \sin \alpha & \cos \alpha \end{pmatrix} \begin{pmatrix} x \\ y \end{pmatrix},$$

where  $\alpha$  is fixed and  $\lambda$  is a parameter.

The origin is always a fixed point and the Jacobian has eigenvalues  $\lambda(\cos \alpha + i \sin \alpha)$ , both have modulus  $|\lambda|$  so they cross the unit circle as  $\lambda$  increases through

one. If we change to polar co-ordinates  $(r, \theta)$  the map becomes

$$\begin{aligned} r_{n+1} &= \lambda r_n - r_n^3 \\ \theta_{n+1} &= \theta_n + \alpha \end{aligned}$$

For  $-1 < \lambda < 1$  the origin is a stable fixed point, but as  $\lambda$  passes through one the origin loses its stability. At the bifurcation point an invariant circle,  $r = \sqrt{\lambda - 1}$ , is created which attracts nearby points. The dynamics on the circle are given by

$$\theta_{n+1} = \theta_n + \alpha.$$

If  $\alpha$  is a rational multiple of  $2\pi$ ,  $\alpha = (p/q)2\pi$ , then the orbit will be periodic with period  $q$ . If  $\alpha$  is an irrational multiple of  $\pi$  then the orbit will not close up. This is called a quasiperiodic orbit.

More generally, a Hopf bifurcation gives rise to an invariant closed curve topologically equivalent to a circle, and the dynamics of the map on this curve can be more complicated than a simple rotation. Higher iterates of the map may undergo Hopf bifurcations, for instance a period  $n$  orbit may give rise to quasiperiodic behaviour on  $n$  tori. As the parameter varies, it is possible for more than one Hopf bifurcation to occur. Such Hopf bifurcations are involved in the various quasiperiodic routes to chaos which have been proposed (Ruelle & Takens, 1971; Newhouse *et al.*, 1978; Curry & Yorke, 1978). These routes to chaos have many universal properties, which have been studied extensively (see Schuster, 1989, for an excellent summary of these). For instance, one feature that is often observed is frequency locking, where the system exhibits periodic behaviour for quite large windows of parameter values.